



HAL
open science

3D application of the coupled criterion to crack initiation prediction in epoxy/aluminum specimens under four point bending

Aurélien Doitrand, Dominique Leguillon

► **To cite this version:**

Aurélien Doitrand, Dominique Leguillon. 3D application of the coupled criterion to crack initiation prediction in epoxy/aluminum specimens under four point bending. *International Journal of Solids and Structures*, In press, 143, 10.1016/j.ijsolstr.2018.03.005 . hal-01741801

HAL Id: hal-01741801

<https://hal.sorbonne-universite.fr/hal-01741801>

Submitted on 23 Mar 2018

HAL is a multi-disciplinary open access archive for the deposit and dissemination of scientific research documents, whether they are published or not. The documents may come from teaching and research institutions in France or abroad, or from public or private research centers.

L'archive ouverte pluridisciplinaire **HAL**, est destinée au dépôt et à la diffusion de documents scientifiques de niveau recherche, publiés ou non, émanant des établissements d'enseignement et de recherche français ou étrangers, des laboratoires publics ou privés.

3D application of the coupled criterion to crack initiation prediction in epoxy/aluminum specimens under four point bending

Aurélien Doitrand¹, Dominique Leguillon²

¹*Safran Aircraft Engines, Rond-point René Ravaut, 77550 Moissy-Cramayel, France
aurelien.doitrand@safrangroup.com*

²*Institut Jean le Rond d'Alembert, CNRS UMR 7190, Sorbonne Universités, UPMC Université Paris 6,
F-75005 Paris, France
dominique.leguillon@upmc.fr*

Abstract

Until now, the coupled stress and energy criterion has mainly been used in 2D applications, but it is possible to extend it to a 3D case. Herein the crack initiation in epoxy/aluminum bimaterial specimens under four point bending is predicted through a 3D numerical application of the coupled criterion. The stress and the energy conditions are computed by means of 3D finite element modeling of both undamaged and cracked specimens. The crack initiates at the epoxy/aluminum interface, meshes of the cracked specimens take into account the crack topology which is determined using the interface normal stress isocontours. By indirect confrontation to experimental tests on aluminum/epoxy bimaterial specimens of different width, the proposed approach allows determining the interface strength and fracture energy. The blind application of the proposed method to a crack initiation in aluminum/epoxy/aluminum specimens of different epoxy layer thickness under four point bending leads to a reasonable agreement with experimental data.

Keywords: Bending, Bimaterial, Crack, Energy release rate, Fracture

1. Introduction

Crack initiation is a main issue in material and structure design. In an industrial process, predictive modeling tools are needed in order to reduce the number of experimental tests that may be costly and time consuming.

An efficient method for crack initiation prediction in brittle materials, the so called "coupled criterion", has been proposed by Leguillon [8]. It is based on the fact that crack nu-

cleation requires two necessary conditions to be fulfilled simultaneously. The first condition is a balance between the energy required to initiate a crack and the one dissipated by the formation of this crack, while the second condition compares the tensile stress to the tensile strength prior to crack initiation.

The coupled criterion has been widely used in order to study fracture initiation. Its efficiency has been demonstrated for various materials through 2D models: for instance composite materials [2, 3, 4, 17, 18, 21], ceramics [12], bimaterial specimens [10], rocks [11], under thermal [9] and/or mechanical [23] loadings. It works also well for interfaces [14, 15] and joints [1, 19]. Various configurations were studied: sharp and blunted V-notched specimens [13], cavities [22], etc. An extensive review about the coupled criterion has been proposed by Weißgraeber *et al.* [24].

Until now, the coupled criterion has mainly been used in 2D applications. It is possible to extend it to some 3D cases, since its formulation holds valid in 3D [10]. However, contrary to 2D cases, where the crack is generally described by only one or two parameters (its length and possibly its direction if unknown), the main difficulty of the 3D case is that the crack may be described by an infinite set of parameters [2, 24]. To the authors knowledge, there are only few 3D applications of the coupled criterion in the literature. Leguillon [10] proposed a 3D extension of the coupled criterion using matched asymptotic expansions, hence under the assumption of a small crack extension. Recently, crack initiation in composite laminates and woven composites [2] has been studied using the coupled criterion and 3D Finite Element (FE) modeling. In both cases, assumptions on the crack shape were made in order to simplify the analysis, preventing the real crack shape determination. A similar approach was used by García *et al.* [4] to predict 3D transverse cracking in laminates.

In this paper, a 3D application of the coupled criterion is proposed that allows determining both the initiation load and the 3D crack shape. The studied case is four point bending of aluminum/epoxy bimaterial specimens [6], which is described in Section 2. A brief recall of the coupled criterion and the crack shape determination method are presented in Section 3. In Section 4, a FE modeling of the four point bending is performed in order to determine crack initiation. In Section 5.1, the interface fracture properties (strength and toughness) are determined by confrontation of the numerical results to experimental data from [6]. In

Section 5.2, the proposed method is applied to study crack initiation under four point bending of specimens composed of two aluminum prisms bonded by a thin epoxy layer [7].

2. Experimental tests and data

The numerical problem under investigation from Section 3 to 5.1 is crack initiation prediction under four point bending of aluminum/epoxy bimaterial specimens. The test configuration and the specimen dimensions are depicted in Figure 1a. Some experimental tests aiming at determining fracture initiation under these conditions were performed by Labossière and Dunn [6] for $w = (4.0, 6.2, 8.9, 12.5$ and $17.5)$ mm width specimens. For the tested configurations, a crack initiates at the bottom epoxy/aluminum interface corner as explained in [6]. Labossière and Dunn determined the failure stress (calculated as the normal stress that would exist at the bottom tip of a homogeneous beam of section $w \times w$ under four-point bending) as a function of the specimen width for both a polished and a bead blasted epoxy/aluminum interface.

In Section 5.2, the same method as presented in the preceding sections is used to study crack initiation in specimens consisting of two prisms of aluminum bonded by a thin epoxy layer (Figure 1b). Numerical predictions of crack initiation stress as a function of the epoxy layer thickness a are confronted to experimental results from Labossière and Dunn [7]. All the experimental data used in this paper for the comparison with numerical results are taken from [6] and [7].

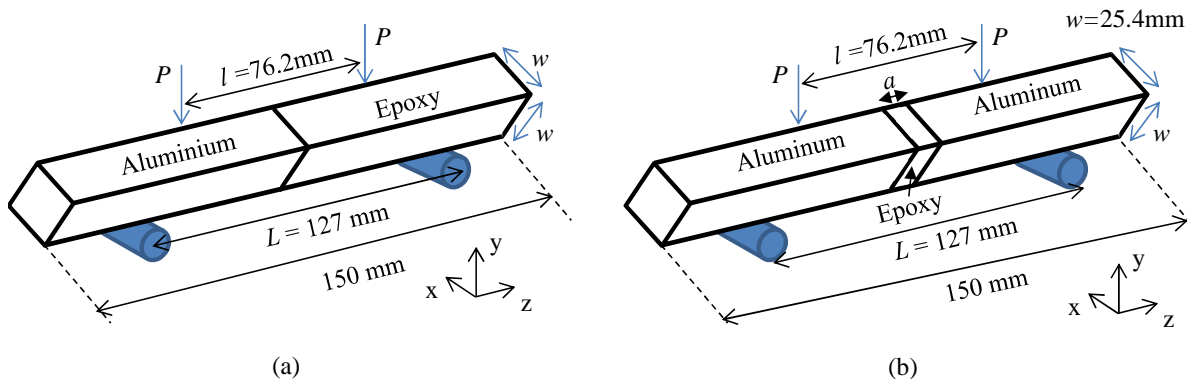


Figure 1: The (a) epoxy/aluminum and (b) aluminum/epoxy/aluminum four point bending test.

3. The coupled criterion for crack initiation prediction

Crack initiation requires the fulfillment of two separate conditions [8]. On the one hand, stress must be high enough to damage the material and on the other hand, sufficient energy is required in order to open the crack. The energy condition states that the incremental energy release rate G^{inc} (*i.e.* the ratio between the change in potential energy W due to crack initiation and **the area S of a crack whose shape is described by a set of parameters $\mathbf{d} = (d_1, \dots, d_n)$**) must be higher than the material fracture energy G^c (Eq. 1). Under the assumption of elasticity, the potential energy of both the damaged and the undamaged material, and hence the incremental energy release rate, are proportional to the square applied load P (Eq. 1). In Eq. (1), A only depends on the specimen geometry (including the crack shape) and mechanical properties.

$$G^{\text{inc}}(S, \mathbf{d}) = \frac{\Delta W}{S} = \frac{W(0) - W(S, \mathbf{d})}{S} = A(S, \mathbf{d}) \cdot P^2 \geq G^c \quad (1)$$

$A(S, \mathbf{d})$ can be determined by generating response surfaces of the potential energy change, ΔW , to the varying set of parameters S and \mathbf{d} by means of finite element calculations with the corresponding cracked configuration [2].

The stress condition states that at crack initiation, the crack surface must be overloaded. In the studied case, it means that the interface normal stress σ_{zz} must be higher than the interface tensile strength σ_c on the whole crack surface defined by S and \mathbf{d} , **prior to initiation**. Under the assumption of elasticity, the stress is proportional to the applied load P (Eq. (2)). Therefore, only one elastic calculation is needed to compute the stress condition.

$$\sigma_{zz} = kP \geq \sigma_c \text{ over the whole surface } S \quad (2)$$

The crack configuration at damage initiation (*i.e.* S and \mathbf{d}) can be determined as the configuration for which both the stress and the energy conditions are satisfied, minimizing the imposed loading. Such a configuration may be determined by combining and solving Eqs.

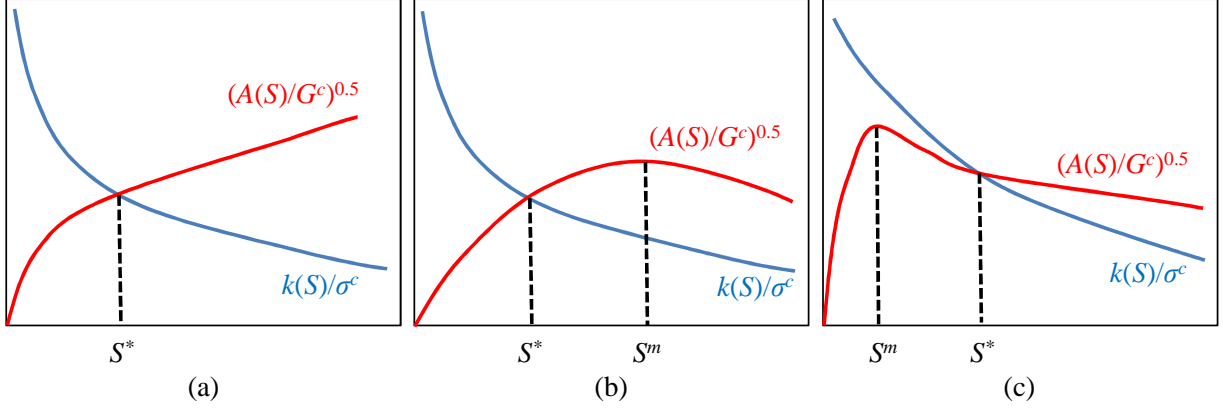


Figure 2: Coupled stress and energy criterion solutions for (a) strictly increasing and (b-c) non-monotonic evolution of A . The solution of Eq. 3 is S^* (a-b) unless A attains a maximum and the energy criterion is the governing condition (c).

(1) and (2) (*cf.* Eq. 3).

$$\frac{A(S, \mathbf{d})}{k^2} = \frac{G^c}{\sigma_c^2} \quad (3)$$

In the following, a method allowing the description of the possible 3D crack shapes by a single parameter is proposed. The initial crack shape is supposed to be plane (it is trivial here because the crack is located at the interface) and to follow the stress isocontours, thus the crack is entirely described by only one parameter: its area S . Therefore, the functions G^{inc} and A only depend on S rather than on a set of parameters \mathbf{d} . Since, in general, k is a decreasing function of S , two main cases may arise in solving the coupled criterion depending on the evolution of A (Figure 2).

In the case where A is a strictly increasing function of S (Figure 2a), it arises that the unique solution S^* of Eq. (3) allows determining not only the crack initiation loading P^* (*cf.* Eq. (4)), but also the crack shape, given by the stress isocontour $\sigma_{zz} = \sigma_c$. In this case, the crack can be parametrized by only one variable (for instance the crack area).

$$P^* = \frac{\sigma_c}{k(S^*)} = \sqrt{\frac{G^c}{A(S^*)}} \quad (4)$$

In some cases (*e.g.*, for the so called "negative geometries" [2, 25, 16]), A is not a strictly increasing function of S and attains a maximum for $S = S^m$ (Figure 2b and c). If the smaller solution S^* of Eq. (3) is smaller than S^m , then the same configuration as explained previously

is obtained. The crack initiates with an area S^* and the crack shape is determined using the corresponding stress isocontour. However, if $S^* > S^c$ (Figure 2c), the crack initiation area is S^c rather than S^* , under the assumption that the crack shape can be deduced from the stress isocontours. Indeed, since the stress criterion is fulfilled for $S = S^*$, it is clear that it is also fulfilled for $S = S^c$. Moreover, the energy criterion is fulfilled for a smaller applied load for $S = S^c$ than for $S = S^*$. Therefore, the configuration for which $S = S^c$ is the configuration fulfilling the energy criterion that minimizes the imposed loading. In this case, it is only the energy criterion that governs crack initiation as explained in [2]. It means that, a priori, the crack shape no longer may be determined using the stress isocontours, but should be determined as the configuration for which the energy criterion is fulfilled and that minimizes the imposed loading among all possible crack configurations [2] while continuing to fulfill the stress condition. In this case, the crack shape determination becomes more complex than in the previous situation if no assumptions are made on the crack shape. A reasonable one is that the crack shape is defined by the stress isocontour encompassing the surface S^m .

4. Four point bending and crack initiation modeling

4.1. Boundary conditions for four point bending modeling

The application of the coupled criterion assumes a linear elastic framework in order to ensure that the elastic energy is proportional to the square imposed load and that the stress is proportional to the imposed load. The full modeling of a four point bending test (including the spans and the loading pins) is non linear due to the contact between the specimen, the spans and the pins. An alternative simplifying way to model the specimen flexion consists in imposing the rotation of the specimen sections located at the spans. Since the studied specimen is composed of two materials in a non-symmetric manner, the rotations of the two sections located at the spans are not equal and can be determined using simple beam theory. In the following, the calculations are made under Euler-Bernoulli's beam theory assumptions, considering the configuration sketched in figure 3. The aluminum and epoxy Young's modulus are respectively E_a and E_e . The bending moment under four point bending as a function of the imposed loading P and the length between the two loading pins l and the supporting

spans L is given in Eq. (5)

$$M(z) = \begin{cases} P \cdot z & (0 \leq z \leq \frac{L-l}{2}) \\ \frac{P \cdot (L-l)}{2} & (\frac{L-l}{2} \leq z \leq \frac{L+l}{2}) \\ P \cdot (L-z) & (\frac{L+l}{2} \leq z \leq L) \end{cases} \quad (5)$$

The section rotation, deduced from (5) is given in Eq. (6).

$$\phi(z) = \begin{cases} \frac{Pz^2}{2E_a I} + \phi_0 & (0 \leq z \leq \frac{L-l}{2}) \\ \frac{P \cdot (L-l)}{2E_a I} \cdot z + \phi_0 - \frac{P \cdot (L-l)^2}{8E_a I} & (\frac{L-l}{2} \leq z \leq \frac{L}{2}) \\ \frac{P \cdot (L-l)}{2E_e I} \cdot z + \phi_0 + \frac{P \cdot (L^2-l^2)}{8E_a I} - \frac{P \cdot (L-l) \cdot L}{4E_e I} & (\frac{L}{2} \leq z \leq \frac{L+l}{2}) \\ \frac{-P \cdot (L-z)^2}{2E_e I} + \phi_0 + \frac{P \cdot (L^2-l^2)}{8I} (\frac{1}{E_a} + \frac{1}{E_e}) & (\frac{L+l}{2} \leq z \leq L) \end{cases} \quad (6)$$

The section rotation $\phi_L = \phi(L)$ can be determined as a function of the section rotation $\phi_0 = \phi(0)$, the applied load P , the specimen dimensions and the elastic property mismatch (Eq. (6)). Then the value of both section rotations at spans are known as a function of the applied load and the specimen characteristics by integration of Eqs. (6) (*cf.* Eqs. (7)).

$$\begin{cases} \phi_0 = \frac{1}{L} \left(\frac{P \cdot (L-l) \cdot (-2L^2 - 2L \cdot l + l^2)}{48E_e I} + \frac{P \cdot (L-l) \cdot (-4L^2 - 4L \cdot l - l^2)}{48E_a I} \right) \\ \phi_L = \frac{1}{L} \left(\frac{P \cdot (L-l) \cdot (4L^2 + 4L \cdot l + l^2)}{48E_e I} + \frac{P \cdot (L-l) \cdot (2L^2 + 2L \cdot l - l^2)}{48E_a I} \right) \end{cases} \quad (7)$$

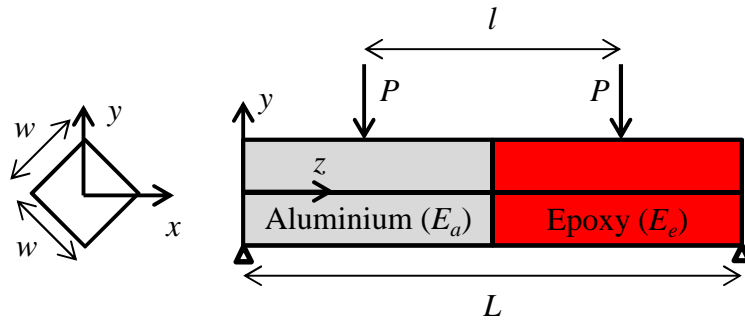


Figure 3: Bimaterial four point bending configuration studied to determine the rotation of the specimen section located at the spans.

In the following, only the specimen part located between the spans is modeled and the applied boundary conditions of the FE models are a rotation of the specimen end sections (located at the spans). Although these boundary conditions are not exactly the same as for the experimental tests, the specimens undergo flexion and a linear elastic framework is ensured. Besides, both the applied displacements on the specimen sections and the stresses are proportional to P , and the elastic energy is proportional to P^2 .

Of course, this could be considered as a rough approximation, knowing that the specimen is not slender enough to rigorously apply Euler-Bernoulli's theory. However, this assumption **seems reasonable** in the context of fracture mechanics where the uncertainties are large.

4.2. Cracked specimen modeling

A FE model of each specimen tested experimentally in [6] ($w = 4.0, 6.2, 8.9, 12.5$ and 17.8 mm) has first been used to determine the interface stress isocontours. Figure 4 shows the normal stress (σ_{zz}) field and isocontours at the epoxy/aluminum interface. The stress isocontour shape obtained numerically is close to the one obtained using an analytical approach [10] for small cracks (*i.e.* which depth is small compared to w). As explained in section 3, the crack initiation shape may be determined from the stress isocontours, so that the crack

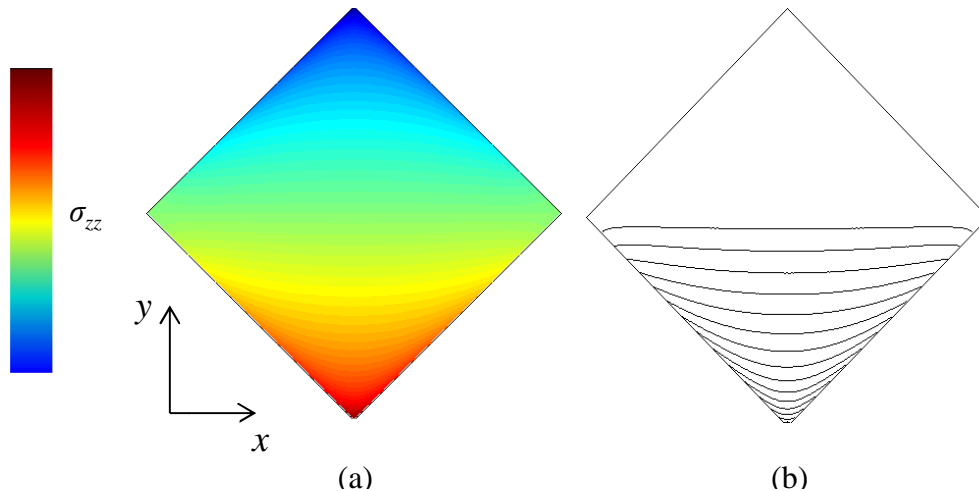


Figure 4: Normal stress (a) field and (b) isocontours at the interface between epoxy and aluminum for a $w = 4.0$ mm width specimen. Stress values are extracted at the nearest Gauss points in the epoxy. The red colour corresponds to a positive (tension) tensile stress whereas the blue one is associated with negative values (compression).

can be described by only one parameter. In order to implement the coupled criterion, it is then necessary to use a specimen mesh with a crack whose shape is based on the stress isocontours at the epoxy/aluminum interface. An automated approach has been carried out in order to obtain such cracked specimen mesh (Figure 5). The stress isocontours are first determined from the elastic calculation on an undamaged specimen. Then, a 2D mesh of the interface including the crack shape is generated (Figure 5a) and extruded in order to obtain the full specimen mesh (Figure 5b), the mesh being refined in the vicinity of the interface. Finally, the nodes of the interface crack are unbuttoned so that the crack can open, which is the only difference between the meshes used to compute $W(S)$ and $W(0)$, hence reducing the numerical errors made on the potential energy change calculation. **The potential energies have been calculated by post-treatment of FE calculations as the weighted sum of the local elastic energy calculated at each Gauss point. A mean mesh size $w/50$ at the aluminum/epoxy interface has been used, ensuring a difference on the computed failure stress lower than 0.1% compared to finer meshes.** For each specimen configuration (with w varying), 15 stress isocontour values have been chosen and the corresponding meshes have been generated in order to compute $W(S)$. The FE calculations have been performed using Zébulon FE solver [26]. The material mechanical properties used are $E_a = 70$ GPa, $\nu_a = 0.33$ for aluminum and $E_e = 2.98$ GPa, $\nu_e = 0.38$ for epoxy [6].

Note that, as underlined in [10], the line where the interface meets the traction free surface is singular, even if less singular than the corner. This means that the associated generalized stress intensity factor of the line singularity is decreasing very strongly and even becoming negative to match with the compressive part. As a consequence the computed isocontours end at that line. It is clear that this approximation is acceptable, although slightly mesh dependent, and gives realistic crack front shapes, since a theoretical line indefinitely approaching the edge is only a mathematical model.

5. Numerical and experimental crack initiation results

5.1. Aluminum-epoxy bi-material specimens

Figure 6a shows the incremental energy release rate G^{inc} (Eq. (1)) as a function of the normalized crack area $\frac{S}{w^2}$ for several values of the specimen width w . Whatever the specimen

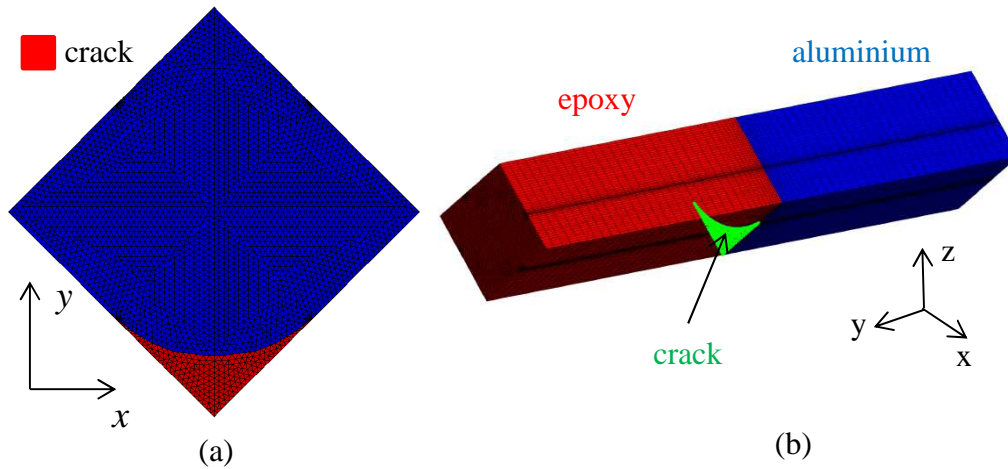


Figure 5: (a) 2D mesh of the aluminum/epoxy interface including the crack shape determined using normal stress isocontours; (b) 3D cracked mesh of an epoxy/aluminum bimaterial specimen obtained by extrusion of the mesh shown in (a).

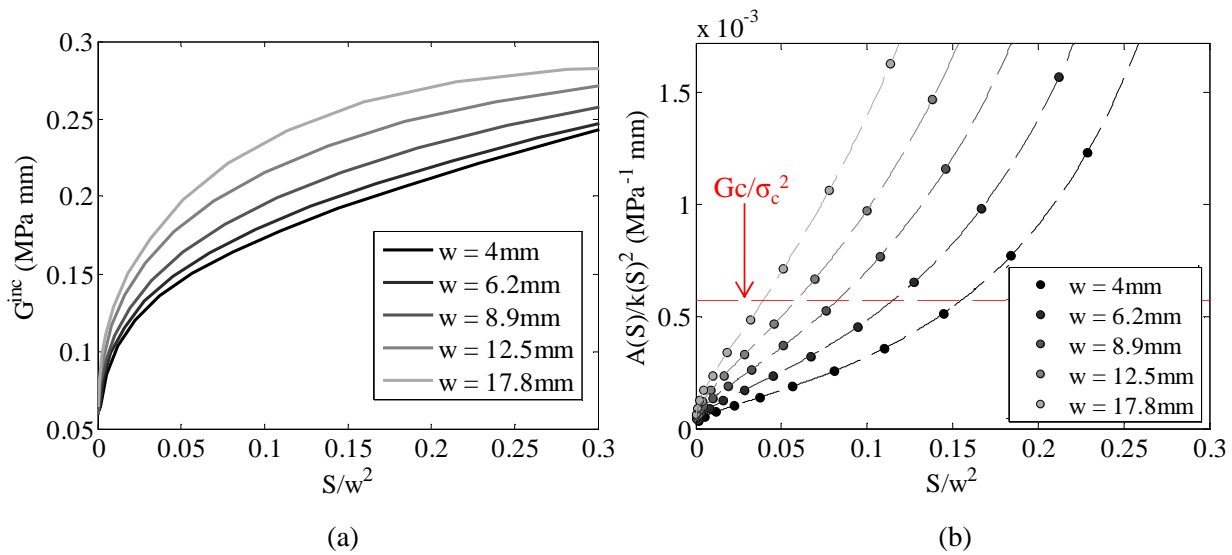


Figure 6: (a) Incremental energy release rate G^{inc} as a function of normalized crack area $\frac{S}{w^2}$ and (b) solution of the coupled criterion (*cf.* Eq. 3) for several specimen width w .

width, the incremental energy release rate is a monotonic increasing function of the crack area. Therefore, as explained in section 3, it is proper to determine the crack shape using the stress isocontour shape. Figure 6b illustrates Eq. (3). The crack initiation area corresponds

to the intersection of $\frac{A(S)}{k(S)^2}$ and $\frac{G^c}{\sigma_c^2}$, given G^c and σ_c , which clearly shows that the higher w , the higher the normalized crack surface at initiation. The critical load is then determined from the initiation crack area S^* using Eq. (4).

The only data missing to implement the coupled criterion are the failure properties of the interface: σ_c and G^c , which are not provided in [6]. The available information in [6] is the tensile strength of the epoxy $\sigma_y = 52$ MPa, which is, as explained in [10], nothing more than an upper bound of the tensile strength of the interface.

The following analysis concerns the determination of the couples (G^c, σ_c) that best fit the experimental results in the case of a polished and a bead blasted interface. For both cases, a couple (G^c, σ_c) has been determined which minimizes the difference between crack initiation stress predictions and experimental results in a least square sense. The following results are obtained:

- o Polished interface : $G^c = 55.0 \cdot 10^{-3}$ MPa mm, $\sigma_c = 9.45$ MPa
- o Bead blasted interface : $G^c = 80.6 \cdot 10^{-3}$ MPa mm, $\sigma_c = 8.90$ MPa

These results indicate that the bead blasted interface is tougher than the polished one, leading to a higher crack initiation stress. This is a conceivable result knowing that the fracture surface is more rugged in this case. Besides, the obtained fracture properties of the interface appear to be within the order of magnitude of both an adhesive bond by means of a polymer [5] and the fracture properties obtained by Leguillon from matched asymptotic expansions and FE calculations [10]. Figure 7 shows the crack initiation stress obtained using the coupled criterion with these parameters as a function of the specimen width in the case of a polished (Figure 7a) and bead blasted (Figure 7b) interface. Even if the fracture parameters have been determined so as to best fit the experimental data, it is clear that the obtained initiation stress trends are qualitatively good, which shows the ability of the coupled criterion to describe the specimen width influence on the crack initiation critical load. The interface initiation cracks corresponding to the different specimen widths are shown in Figure 8.

5.2. Aluminum-epoxy-aluminum specimens

The same approach as presented in sections from 3 to 5.1 has been used in order to determine crack initiation under four point bending of specimens composed of two aluminum

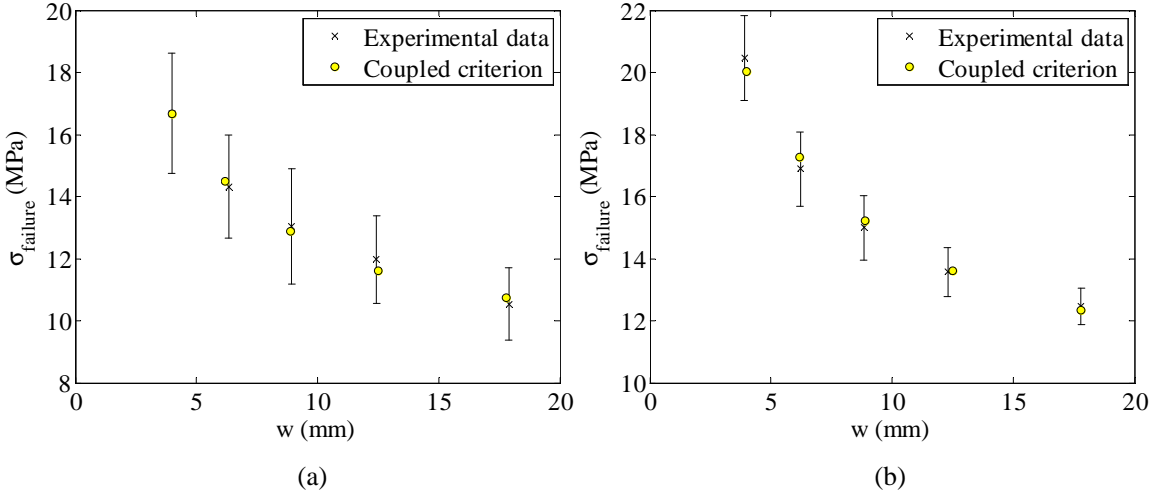


Figure 7: Comparison between experimental data from [6] and numerical results obtained using the coupled criterion for a (a) polished and (b) bead blasted interface using respectively the fracture parameters (a) ($G^c = 55.0 \cdot 10^{-3} \text{ MPa mm}$, $\sigma_c = 9.45 \text{ MPa}$) and (b) ($G^c = 80.6 \cdot 10^{-3} \text{ MPa mm}$, $\sigma_c = 8.90 \text{ MPa}$)

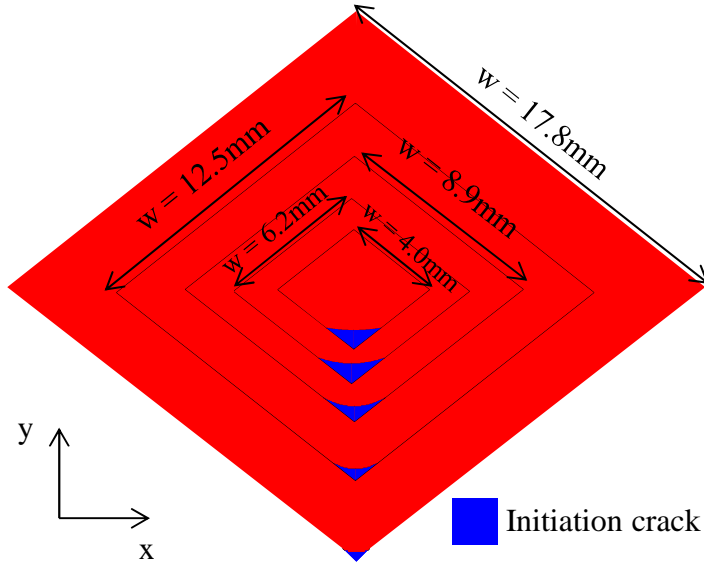


Figure 8: Interface initiation cracks (in blue) for different value of specimen width w (the results have been superimposed for visualization purpose).

prisms bonded by a thin epoxy layer (Figure 1b) for different epoxy layer thicknesses (in the case of polished interfaces). Similarly to the first studied case, the applied boundary conditions are rotations of the specimen sections located at the spans. Contrary to the bimaterial case, this configuration is symmetric with respect to the specimen middle section.

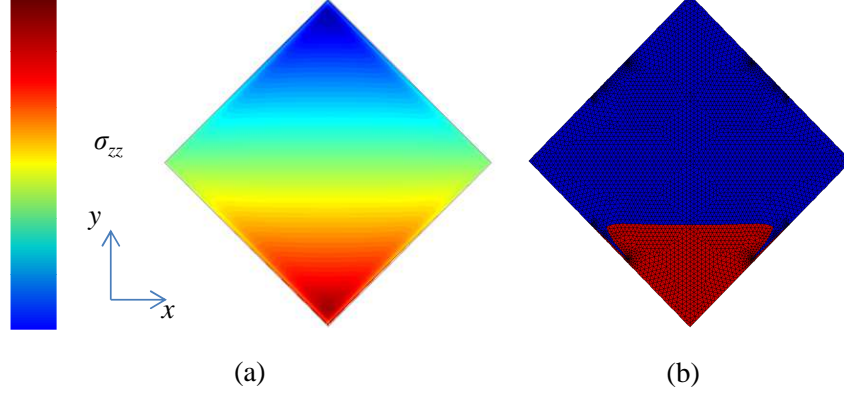


Figure 9: (a) Interface normal stress field and (b) 2D interface mesh taking into account a crack whose shape is determined using a stress isovalue.

The rotation angles ϕ_0 and ϕ_L can be determined as a function of the applied loading P and the specimen characteristics (Eq. (8)).

$$\phi_0 = -\phi_L = \frac{P \cdot (L - l)^2}{8E_a \cdot I} - \frac{P \cdot (L - l)}{4I} \left(\frac{L - a}{E_a} + \frac{a}{E_e} \right) \quad (8)$$

The interface normal stress isocontour shapes are slightly more complex than for the first studied case (Figure 9a). Nevertheless, it does not trigger much more difficulties to generate an interface mesh including the crack topology (Figure 9b). The FE calculations have been performed using meshes with an epoxy layer $a = 0.1, 0.2, 0.4, 0.6, 0.8$ and 1.1 mm thick and containing at least 6 elements in the epoxy thickness. The symmetry of the studied configuration raises the question whether damage initiates at only one or both aluminum-epoxy interfaces. The incremental energy release rate as a function of the normalized crack surface $\frac{S}{n \cdot w^2}$ (n being the number of cracks) is presented in Figure 10 for an epoxy layer $a=0.1$ mm thick (Only one case is shown for visualization purpose, the same conclusions being obtained for other values of a). The incremental energy release rate associated to the initiation of a single crack is higher than that associated to the initiation of two cracks, whatever the crack normalized area. This is likely due to a shielding effect. Therefore, we conclude that damage initiates at only one interface rather than two. This result is supported by experimental tests from Labossière and Dunn [7], who showed experimentally that only one interface is damaged at crack initiation. It can be noted that the incremental energy release rate attains a maximum, which may cause difficulties in the crack shape determination

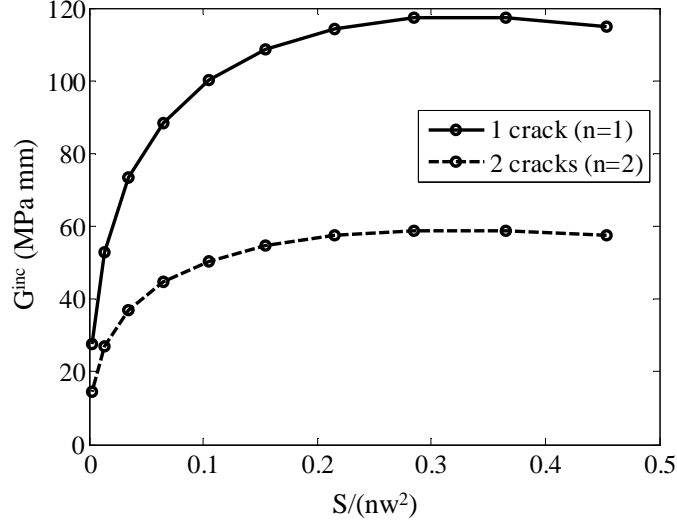


Figure 10: Incremental energy release rate associated to the initiation of a single or two cracks as a function of the normalized cracked surface for an epoxy layer 0.1mm thick.

in some cases (*cf.* Section 3).

The initiation stress as a function of the epoxy layer thickness obtained applying the coupled criterion is shown in Figure 11 using respectively the fracture parameters obtained in the first analysis for a polished interface ($G^c = 51.0 \cdot 10^{-3}$ MPa mm, $\sigma_c = 9.45$ MPa, Figure 11a) and those who best fits experimental data ($G^c = 44.0 \cdot 10^{-3}$ MPa mm, $\sigma_c = 6.43$ MPa, Figure 11b). In both cases, the coupled criterion resolution leads to the case presented in Figure 2b whatever the epoxy layer thickness. **Therefore, the case presented in Figure 2c, for which the crack shape may not be determined using the stress isocontours, is not encountered herein**

Similarly to the case of bimaterial specimens, the coupled criterion is able to qualitatively catch the influence of the epoxy layer on the initiation stress. The initiation stress evolution as a function of the epoxy thickness shows a reasonable agreement with experimental data using the fracture parameter couple determined in the first analysis, even if it seems to slightly overestimate the initiation stress compared to experimental data for the thickest epoxy layers. The observed difference may be explained by the fact that for aluminum-epoxy specimens the epoxy part is a bulk material whereas it is a thin layer in the case of the aluminum-epoxy-aluminum specimens, leading to a possible slightly different behavior. In

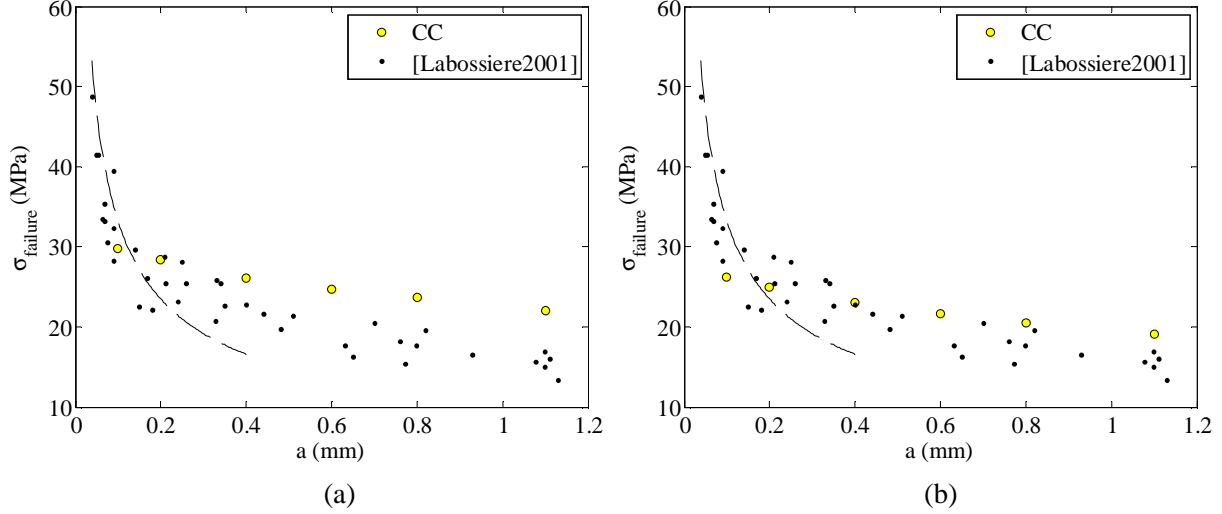


Figure 11: Crack initiation stress as a function of the epoxy layer thickness a obtained using the fracture parameters (a) determined in the case of the bimaterial specimens ($G^c = 51.0 \cdot 10^{-3} \text{MPa}\cdot\text{mm}, \sigma_c = 9.45$) and (b) that best fit experimental results ($G^c = 44.0 \cdot 10^{-3} \text{MPa}\cdot\text{mm}, \sigma_c = 6.43 \text{MPa}$). The dashed line corresponds to the asymptotic behavior [20] for very small layer thicknesses.

particular, it must be ensured that the epoxy has correctly filled the small space separating the two aluminum parts.

On the contrary, it seems difficult to capture the dramatic increase of the tensile stress at failure for the smallest thicknesses. It is shown in a 2D asymptotic model [20] that it grows like $1/\sqrt{a}$ (see Figure 11) while being obviously bounded by the aluminum resistance. A possible explanation for the discrepancy observed between numerical and experimental results for really small interfaces is the interface exhibiting a non-linear cohesive behavior, which has not been taken into account in the present model. Likely, such a big slope is rather difficult to represent using FE computations with a limited number of elements in the thickness of the adhesive layer, especially in 3D computations.

6. Conclusion

The proposed approach, which is a 3D numerical application of the coupled criterion to epoxy/aluminum bimaterial four point bending, allows the crack initiation shape and loading to be predicted. The crack shape is determined using the interface stress isocontours, which is a rigorous approach within the framework of the coupled criterion if the incremental energy

release rate is a monotonic increasing function of the crack area. The advantage of such a method is that the 3D crack can be parameterized by only one variable. However, determining the crack shape using the stress isocontours is not always valid, especially if the incremental energy release rate has a maximum and if the energy criterion is dominant relatively to the stress criterion. In these cases, the crack shape must be determined using the energy criterion only, which could become much more costly from the numerical point of view.

Since the failure properties (tensile strength and toughness) of the interface were not known, the proposed approach can be employed as an inverse method to determine G^c and σ_c by comparing the numerical results to the experimental data. Experiments by Labossière and Dunn [6] were used but they do not allow a direct confirmation of the approach since some data lack. Even if the confirmation is not direct, the obtained results may indicate the consistency of the approach in a 3D case. Indeed, the coupled criterion qualitatively gives a good trend of the critical crack initiation load as a function of the bimaterial specimen width. Moreover, it is found that the bead blasted interface is tougher than the polished one as expected, leading to a higher crack initiation stress. Finally, the obtained properties of the interface appear to be within the order of magnitude of an adhesive bond by means of a polymer.

The blind application of the proposed method to crack initiation prediction in specimens made of two aluminum prisms bonded by a thin epoxy layer using the fracture parameters determined in the case of the aluminum-epoxy bimaterial specimens leads to a reasonable agreement with experimental data. The initiation stress evolution prediction is qualitatively similar to experimental data and slightly overestimated compared to experimental data for the thickest layers. The observed difference may be explained by interfaces (in the case of an aluminum-epoxy specimen and of an aluminum-epoxy-aluminum specimen) not having exactly the same adhesion properties because of the difference in geometries that could lead to different conditions of making the specimens. They may also be explained by the chosen boundary conditions, that are convenient for applying the coupled criterion but may not represent exactly those of the experimental test.

The proposed approach deals with a 3D crack initiating in a plane at aluminum/epoxy interface. In other 3D cases, the crack shape may be more complex (*e.g.*, a 3D surface). If

the possible crack surfaces are known, the crack shape may be determined using the stress isocontours over these surfaces, unless the energy criterion is dominant relatively to the stress criterion. The case when the crack plane or surface is not known may lead to further investigations so as to determine it before applying the proposed method.

References

- [1] Carrère, N., Martin, E., Leguillon, D., 2015. Comparison between models based on a coupled criterion for the prediction of the failure of adhesively bonded joints *Engng. Fract. Mech.* 138, 185-201.
- [2] Doitrand, A., Fagiano, C., Carrère, N., Chiaruttini, V., Hirsekorn, M., 2017. Damage onset modeling in woven composites based on a coupled stress and energy criterion. *Engng. Fract. Mech.* 169, 189-200.
- [3] [García, I.G., Paggi M., Mantič V., 2014. Fiber-size effects on the onset of fiber-matrix debonding under transverse tension: A comparison between cohesive zone and finite fracture mechanics models. *Engineering Fracture Mechanics* 115, 96-110.](#)
- [4] García, I.G., Carter, B.J., Ingrassia, A.R., Mantič V., 2016. A numerical study of transverse cracking in cross-ply laminates by 3D finite fracture mechanics. *Composites Part B: Engineering* 95, 475-487.
- [5] Krishnan, A., Xu L.R., 2011. Systematic evaluation of bonding strengths and fracture toughnesses of adhesive joints. *J. of Adhesion* 87, 1-19.
- [6] Labossière, P.E.W., Dunn, M.L., 2001. Fracture initiation at three-dimensional bimaterial interface corners. *J. Mech. Phys. of Solids* 49 (3), 609-634.
- [7] Labossière, P.E.W., Dunn, M.L., 2001. Prediction of fracture initiation at three-dimensional bimaterial interface corners: application to butt-joints loaded in bending. In *Proceedings of International Conference on Fracture (ICF 10) 2001, Hawaii*.
- [8] Leguillon, D., 2002. Strength or toughness? A criterion for crack onset at a notch. *Eur. J. Mech. - A/Solids* 21 (1), 61-72.
- [9] Leguillon, D., 2013. A simple model of thermal crack pattern formation using the coupled criterion. *Comptes Rendus Mécanique* 341 (6), 538-546.
- [10] Leguillon, D., 2014. An attempt to extend the 2D coupled criterion for crack nucleation in brittle materials to the 3D case. *Theor. Appl. Fract. Mech.* 74, 7-17.

- [11] Leguillon, D., Karneeva, E., Baroni, A., Putot, C., 2013. Tight sedimentary covers for CO₂ sequestration. *Int. J. Fract.* 184(1), 113-122.
- [12] Leguillon, D., Martin, E., Ševeček, O., Bermejo, R., 2015. Application of the coupled stress-energy criterion to predict the fracture behaviour of layered ceramics designed with internal compressive stresses. *Eur. J. Mech. - A/Solids* 54, 94-104.
- [13] Leguillon, D., Quesada, D., Putot, C., Martin, E., 2007. Size effects for crack initiation at blunt notches or cavities. *Engng. Fract. Mech.* 74, 2420-2436.
- [14] Mantič, V., 2009. Interface crack onset at a circular cylindrical inclusion under a remote transverse tension. Application of a coupled stress and energy criterion. *Int. J. Solids Structures* 46, 1287-1304.
- [15] Mantič, V., García, I.G., 2012. Crack onset and growth at the fibre-matrix interface under a remote biaxial transverse load. Application of a coupled stress and energy criterion. *Int. J. Solids Structures* 49, 2273-2290.
- [16] Martin, E., Leguillon, D., 2004. Energetic conditions for interfacial failure in the vicinity of a matrix crack in brittle matrix composites. *Int. J. Solids Structures* 41, 6937-6948.
- [17] Martin, E., Leguillon, D., Carrère, N., 2010. A twofold strength and toughness criterion for the onset of free-edge shear delamination in angle-ply laminates. *Int. J. Solids and Structures* 47 (9), 1297-1305.
- [18] Martin, E., Leguillon, D., Carrère, N., 2012. A coupled strength and toughness criterion for the prediction of the open hole tensile strength of a composite plate. *Int. J. Solids and Structures* 49 (26), 3915-3922.
- [19] Moradi, A., Carrère, N., Leguillon, D., Martin, E., Cognard, J.Y., 2013. Strength prediction of bonded assemblies using a coupled criterion under elastic assumptions: Effect of material and geometrical parameters. *Int. J. Adhesion and Adhesives* 47, 73-82.
- [20] Nguyen, L.M., Leguillon, D., Gillia, O., Riviere, E., 2012. Bond failure of a SiC/SiC brazed assembly. *Mechanics of Materials* 50, 1-8.

- [21] Reinoso, J., Arteiro, A., Paggi, M., Camanho, P.P., 2017. Strength prediction of notched thin ply laminates using finite fracture mechanics and the phase field approach. *Composites Science and Technology* 150, 205-216.
- [22] Romani, R., Bornert, M., Leguillon, D., Le Roy, R., Sab, K., 2015. Detection of crack onset in double cleavage drilled specimens of plaster under compression by digital image correlation. *Eur. J. mech. A/Solids* 51, 172-182.
- [23] Rosendahl, P.L., Weißgraeber, P., Stein, N., Becker, W., 2017. Asymmetric crack onset at open-holes under tensile and in-plane bending loading. *Int. J. Solids and Structures* 113, 10-23.
- [24] Weißgraeber, P., Leguillon, D., Becker, W., 2016. A review of Finite Fracture Mechanics: crack initiation at singular and non-singular stress raisers. *Archive Appl. Mech.* 86 (1-2), 375401.
- [25] Weißgraeber, P., Hell, S., Becker, W., 2016. Crack nucleation in negative geometries, *Engng. Fract. Mech.* 168, 93-104.
- [26] <http://www.zset-software.com/products/zebulon/>